Weldability Study of Tungsten Inert Gas Welded Al-8%SiC Metal Matrix Composite Using Response Surface Methodology

Pritam Singh[1], Md. Taslim[2], Soumojit Dasgupta[3]*, Sumanta Chatterjee[4]
[1-3]*Mechanical Engineering Department & JIS College of Engineering*
[4]*Computer Science Engineering Department & JIS College of Engineering*

**soumojit.dasgupta@jiscollege.ac.in*

---***---

Abstract - Over the years Metal Matix Composite (MMC) has developed into a very essential material for modern manufacturing processes. Particularly aluminium based MMCs have a widespread importance due to their physical and chemical properties which make them applicable for aviation and aerospace industries. Manufacturing and processing in these industries involve joining procedures, wherein welding plays a primary role. This paper investigates on the weldability of Al-8%SiC MMC by using Tungsten Inert Gas (TIG) welding process. Autogeneous bead on plate TIG welding was performed using argon (99.99% pure) as shielding gas. The factors of Heat Input (kJ/mm), Gas flow rate (lt/min) and Weld Torch Angle (degree) were considered as the input parameters with three levels each. These parameters have considerable effect on the weldability of the base material. In welding, the Bead Geometry (depth of penetration, height of reinforcement and bead width) of the weld bead is a salient feature in welded components. It has a considerable effect on mechanical properties of the weld. The effects of heat input, gas flow rate and weld torch angle on bead geometry were investigated. Central Composite Design of Response Surface Methodology was used as the Design of Experiment for formation of the experimental array. Experimental plots for each bead geometry entities were performed using Minitab 16 software. Also, the effect of individual factors on responses was examined by Analysis of Variance (ANOVA). Optimal weld condition was obtained at heat input of 0.510 kJ/mm, gas flow rate of 14 l/min and weld torch angle of 45º. The corresponding depth of penetration being 1.768 mm, bead width of 3.013 mm and height of reinforcement of 0.114 mm.

Key Words: Weldability, Metal matrix composite, Aluminium, Bead geometry, Response Surface Methodology

1.INTRODUCTION

Aluminium alloys have wide application for fabrication. However, it is getting substituted by aluminium-based composites in components, e.g., drive shafts; hydraulic cylinders etc. for higher weight reduction and improved resistance to wear [1]. Aluminium is a widely used metal matrix material in metal matrix composites and Silicon Carbide (AlSiC), is a commonly used reinforcement [2]. The aluminium silicon carbide composite material has excellent wear resistance [3] and high strength to weight ratio [4].

The most common manufacturing process of aluminium silicon carbide (Al-SiC) composite is Stir Casting because of its high production rate [5]. It is more suitable and economical process in manufacturing Al-SiC MMC compared to Powder Metallurgy [6]. But there are certain drawbacks like poor fracture toughness and ductility [7].

Joining process of aluminium based composites, especially Al-SiC MMC have been a challenge over the years. Welding has always been a major joining procedure. Among the various welding methods, Tungsten Inert Gas (TIG) welding or Gas Tungsten Arc Welding (GTAW) has been found to be very effective in joining Al-SiC based composites. Several research works have been performed on TIG welding of the composite [8-12].

Jayashree et. al [13] investigated on TIG welding of SiC reinforced aluminium metal matrix composites. Thermal ageing operation was performed on some welded components. Microstructure analysis was performed and comparison was made between aged and non-aged weldments. Variations existed w.r.t. micro-orientation and grain boundary. Refinement in grain size was observed in aged weldments. Logsdon and Liaw [14] compared the properties between SiC reinforced aluminium metal matrix composites and wrought aluminium alloys. The former was more lustrous owing to improved strength, stiffness, corrosion attributes, creep and wear resistance. However, limitations include poor ductility and fracture toughness.

Phenomenon and effect of clustering on mechanical properties of Al 2024–SiC metal matrix composite (MMC) powders produced by centrifugal casting was investigated by Hong et. al [15]. Fracture toughness and tensile tests were performed on the MMC materials with varying percentage of SiC. The strength of MMC was proposed to be inferred from load transfer model approach involving cluster mechanism.

Saini et. al [16] made an interesting experimental investigation where the usage of rice husk ash was made in preparing metal matrix composite. It was observed that density of composite decreased and hardness and tensile strength reduced with addition of rice husk ash. TIG welding was performed on AA 6063 aluminium alloy reinforced with 10% rice husk ash to study weldability. Mechanical tests were conducted. The composite with 10% rice husk ash was found satisfactory to be welded.

Pulsed DC TIG welding was performed on Al3Zr/A356 particle-reinforced aluminium matrix composites with 3% particle content by Li et. al [17]. The composite was prepared by in-situ process. Effect of welding variables on microstructure, microhardness and corrosion resistance were investigated. Optimal condition was obtained at 15 kHz pulse frequency and 200 A pulse peak current. At this condition the weld bead was uniform and the reinforcement evenly distributed. Hardness of weld bead increased by 35% compared to parent metal.

Weldability study of TIG welding on AA6061 aluminium alloy was performed by Bansal et. al [18]. Welding was performed in four passes using MGS 525/409 as filler material and argon as shielding gas. Also, mechanical properties like hardness and tensile strength were measured. Microstructure of weld bead was studied. It revealed fine and equiaxed grains at the weldment. Optimal weld condition was obtained at weld current of 190A.

In this experimental investigation, TIG welding of Al-8%SiC metal matrix composite was performed to study weldability of the composite. Input factors considered were heat input (kJ/mm), gas flow rate (lt/min) and weld torch angle (degree). Autogeneous bead on plate TIG welding was performed using Argon (99.9% pure) as the shielding gas. Thoriated tungsten was used as electrode material. Bead geometry parameters (depth of penetration, bead width and height of reinforcement) were examined. Design of experiment used was Central Composite Design of Response Surface Methodology (RSM) [20]. Influence of each factor on bead geometry was analyzed using Analysis of Variance (ANOVA).

2. Experimental Procedure

2.1 Welding Process Parameters

Input factors considered for Tungsten Inert Gas Welding of Al-8%SiC metal matrix composite were-

i) Heat input (kJ/mm)
ii) Gas flow rate (lt/min)
iii) Weld torch angle (degree)

Operating Limits of Input Factors-

Bead on plate TIG welding was performed on Al-8%SiC MMC using 99.9% pure Argon as the shielding gas. Trial runs were performed to finalise the operating limits of the input factors. The following are the operating limits of the factors as shown in Table 1.

Table -1: Input Factors with Levels

Factors	Level 1 (-1)	Level 2 (0)	Level 3 (+1)
Heat input (kJ/mm)	0.389	0.462	0.510
Gas flow rate (lt/min)	10	12	14
Weld torch angle (degree)	45	60	75

2.2 Design matrix of experimentation

The design of experiment and the input variable values according to Response Surface Methodology (RSM) of Central Composite Design (CCD) is shown in Table 2.

Table -2: Design of Experiment Matrix

Sl. No.	Run order	Heat input (kJ/mm)	Gas flow rate (lt/min)	Weld torch angle (degree)
1	9	0.389	10	45
2	18	0.510	10	45
3	12	0.389	14	45
4	10	0.510	14	45
5	11	0.389	10	75
6	17	0.510	10	75
7	6	0.389	14	75
8	1	0.510	14	75
9	20	0.389	12	60
10	8	0.510	12	60
11	19	0.462	10	60
12	7	0.462	14	60
13	16	0.462	12	45
14	2	0.462	12	75
15	3	0.462	12	60
16	13	0.462	12	60
17	15	0.462	12	60
18	5	0.462	12	60
19	14	0.462	12	60
20	4	0.462	12	60

2.3 Experimentation

At first, trial runs were performed on Al-8%SiC metal matrix composites to finalize the limits of the input factors. The following parameters of the TIG welding were considered-

i) Open circuit current – 100A, 120A, 140A
ii) Closed circuit voltage – 10.6V, 11.2V, 11.3V

A total of 20 (twenty) number of samples of size 100mm x 50mm x 10 mm were bead on plate TIG welded using Argon (99.99% purity) without a filer metal. A constant welding speed of 2.18 mm/s was maintained throughout the experiment. *Thoriated tungsten* of diameter 3.2 mm was used as the *electrode material.*

Specification of TIG welding machine-

Make- KEMPPI
Current Range- 80-200 A
Voltage capability- Varies depending on the selected current setting

Cross-section of the samples were cut and then polished on Belt grinders and finished on velvet grinders. *Etching* operation was performed on each sample using *Keller's Reagent* prior to measurement of Bead geometry.

3. Results and Discussion

Bead on plate TIG welding (autogenous) was performed on Al-8%SiC MMC samples. Some of the typical samples are shown in Table 3.

Table -3: Typical bead on plate TIG welded samples

Sl. No.	Heat input (kJ/mm)	Gas flow rate (lt/min)	Weld torch angle (°)	Built Part	Remarks
1	0.389	10	45	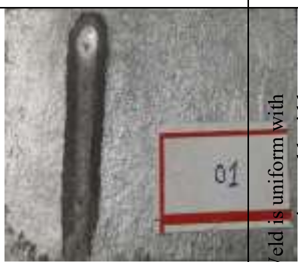	Weld is uniform with increasing weld width towards the end. There are four blow holes on the surface.
2	0.462	14	60		Weld is uniform with few pinholes at the middle.

Bead geometry (depth of penetration, height of reinforcement and bead width) is an important feature in the welding process. In this experimental work, bead geometry of each weldment was measured and the individual effect of each input factor on the bead geometry was studied. Following are the detailed analysis of each bead geometry parameters.

3.1 Depth of Penetration

Depth of penetration is one of the most prime responses in welding process. The objective is to obtain maximum depth of penetration of the weld material. The depth of penetration for each combination of the input factors was measured. The detailed measurements are depicted in Table 4 and Table 5.

Table -4: Measured values of Depth of Penetration

Sl. No.	Arc Current (A) OCC	CCC	Weld voltage (V)	Weld speed (mm/s)	Heat input (kJ/mm)	Gas flow rate (lt/min)	Weld torch angle (degree)	Depth of Penetration
1	100	102	10.6	2.18	0.389	10	45	1.140
2	140	141	11.3	2.18	0.510	10	45	1.253
3	100	101	10.6	2.18	0.389	14	45	1.319
4	140	142	11.3	2.18	0.510	14	45	1.768
5	100	100	10.6	2.18	0.389	10	75	1.566
6	140	141	11.3	2.18	0.510	10	75	1.887

Table-5: Measured values of Depth of Penetration

Sl. No.	Arc Current (A)		Weld voltage (V)	Weld speed (mm/s)	Heat input (kJ/mm)	Gas flow rate (lt/min)	Weld torch angle (degree)	Depth of Penetration (mm)
	OCC	CCC						
7	100	101	10.6	2.18	0.389	14	75	1.460
8	140	142	11.3	2.18	0.510	14	75	1.932
9	100	100	10.6	2.18	0.389	12	60	1.446
10	140	141	11.3	2.18	0.510	12	60	1.633
11	120	122	11.2	2.18	0.462	10	60	1.626
12	120	121	11.2	2.18	0.462	14	60	1.760
13	120	1211	11.2	2.18	0.462	12	45	1.325
14	120	121	11.2	2.18	0.462	12	75	1.732
15	120	121	11.2	2.18	0.462	12	60	1.436
16	120	122	11.2	2.18	0.462	12	60	1.531
17	120	121	11.2	2.18	0.462	12	60	1.583
18	120	121	11.2	2.18	0.462	12	60	1.602
19	120	122	11.2	2.18	0.462	12	60	1.673
20	120	121	11.2	2.18	0.462	12	60	1.587

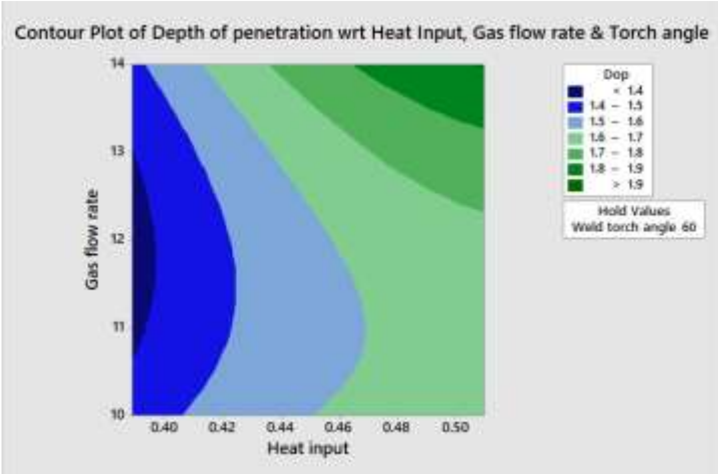

Fig -1: Contour Plot for Depth of Penetration

Contour plot of depth of penetration is shown in Figure 1. Weld torch angle was kept constant at 60º. It was observed that maximum depth of penetration was obtained at heat input within 0.47-0.51 kJ/mm and gas flow rate of 13-14 lt/min. According to Tables 4 and 5, maximum depth of penetration of 1.932 mm was obtained at 0.510 kJ/mm and gas flow rate of 14 lt/min.

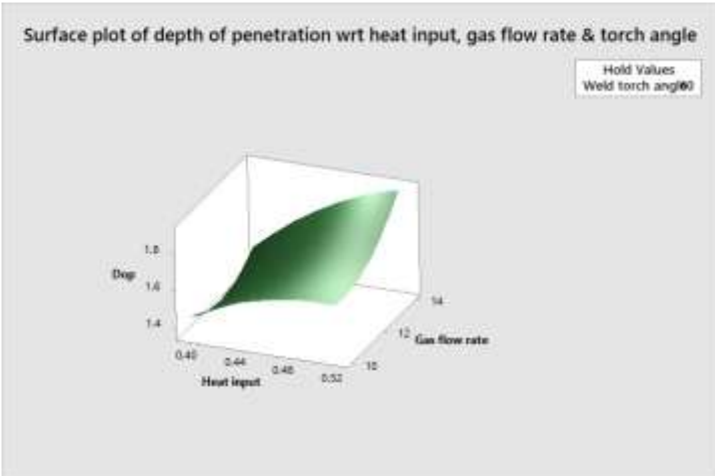

Fig -2: Surface Plot for Depth of Penetration

Surface plot of depth of penetration is shown in Figure 2. Weld torch angle was kept constant at 60º. It is observed that depth of penetration increases from 0.4 kJ/mm onwards and reaches a maximum at 0.45-0.51 kJ/mm. For gas flow rate, depth of penetration increases from 10 lt/min and then gradually increases till 14 lt/min. Maximum depth of penetration of above 1.9 mm was obtained within range of heat input 0.47-0.51 kJ/mm and gas flow rate of range 13.5-14 lt/min.

Analysis of Variance (ANOVA) was performed in measuring contribution of each input parameter on depth of penetration as shown in Table 6.

International Journal of Scientific Research in Engineering and Management (IJSREM)
Volume: 09 Issue: 06 | June - 2025 SJIF Rating: 8.586 ISSN: 2582-3930

Table-6: ANOVA Table of Depth of Penetration

Source	DF	Adj SS	Adj MS	F-Value	P-Value
Model	9	0.756647	0.084072	16.81	0.000
Linear	3	0.610604	0.203535	40.69	0.000
Heat input	1	0.237776	0.237776	47.54	0.000
Gas flow rate	1	0.058829	0.058829	11.76	0.006
Weld torch angle	1	0.313998	0.313998	62.77	0.000
Square	3	0.038474	0.012825	2.56	0.113
Heat input*Heat input	1	0.009691	0.009691	1.94	0.194
Gas flow rate*Gas flow rate	1	0.024370	0.024370	4.87	0.052
Weld torch angle*Weld torch angle	1	0.013615	0.013615	2.72	0.130
2-Way Interaction	3	0.107569	0.035856	7.17	0.007
Heat input*Gas flow rate	1	0.029646	0.029646	5.93	0.035
Heat input*Weld torch angle	1	0.006670	0.006670	1.33	0.275
Gas flow rate*Weld torch angle	1	0.071253	0.071253	14.24	0.004
Error	10	0.050020	0.005002		
Lack-of-Fit	5	0.018463	0.003693	0.59	0.715
Pure Error	5	0.031557	0.006311		
Total	19	0.806667			

Model Summary: R-sq: 93.80%

It was observed that both heat input and weld torch angle with P-values of 0.000 (<0.05) each have considerable effect on depth of penetration. This is followed by gas flow rate with a P-value of 0.006, which is also <0.05. Also, the R-sq value of 93.80 % indicates that the model is a good fit.

3.2 Height of Reinforcement

The height of reinforcement for each combination of the input factors was measured. The height is recommended to be positive on the nominal side. The detailed measurements are depicted in Table 7 and Table 8.

Table -7: Measured values of Height of Reinforcement

Sl. No.	Arc Current (A)		Weld voltage (V)	Weld speed	Heat input (kJ/mm)	Gas flow rate (lt/min)	Weld torch angle (degree)	Height of Reinforcement
	OCC	CCC						
1	100	102	10.6	2.18	0.389	10	45	0.066
2	140	141	11.3	2.18	0.510	10	45	0.083
3	100	101	10.6	2.18	0.389	14	45	0.074
4	140	142	11.3	2.18	0.510	14	45	0.114
5	100	100	10.6	2.18	0.389	10	75	0.122
6	140	141	11.3	2.18	0.510	10	75	0.128

Table -8: Measured values of Height of Reinforcement

Sl. No.	Arc Current (A)		Weld voltage (V)	Weld speed (mm/s)	Heat input (kJ/mm)	Gas flow rate (lt/min)	Weld torch angle (degree)	Depth of Penetration (mm)
	OCC	CCC						
7	100	101	10.6	2.18	0.389	14	75	0.105
8	140	142	11.3	2.18	0.510	14	75	0.144
9	100	100	10.6	2.18	0.389	12	60	0.112
10	140	141	11.3	2.18	0.510	12	60	0.123
11	120	122	11.2	2.18	0.462	10	60	0.115
12	120	121	11.2	2.18	0.462	14	60	0.118
13	120	1211	11.2	2.18	0.462	12	45	0.084
14	120	121	11.2	2.18	0.462	12	75	0.124
15	120	121	11.2	2.18	0.462	12	60	0.118
16	120	122	11.2	2.18	0.462	12	60	0.102
17	120	121	11.2	2.18	0.462	12	60	0.106
18	120	121	11.2	2.18	0.462	12	60	0.108
19	120	122	11.2	2.18	0.462	12	60	0.109
20	120	121	11.2	2.18	0.462	12	60	0.98

International Journal of Scientific Research in Engineering and Management (IJSREM)
Volume: 09 Issue: 06 | June - 2025 SJIF Rating: 8.586 ISSN: 2582-3930

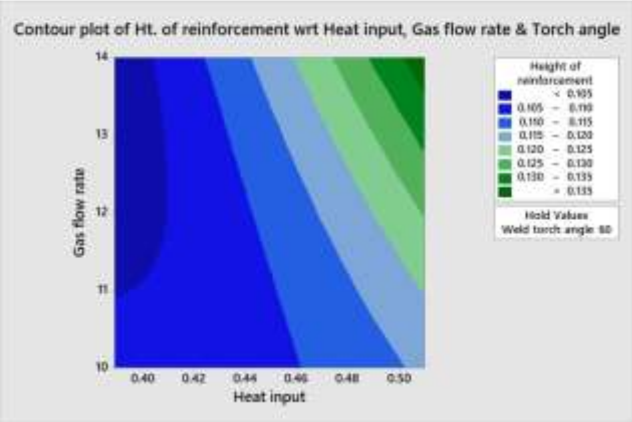

Fig -3: Contour Plot for Height of Reinforcement

Contour plot of height of reinforcement is shown in Figure 3 at constant weld torch angle of 60º. It was observed that nominal (minimum) height of reinforcement was obtained at heat input within 0.41 kJ/mm and gas flow rate of 11-14 lt/min.

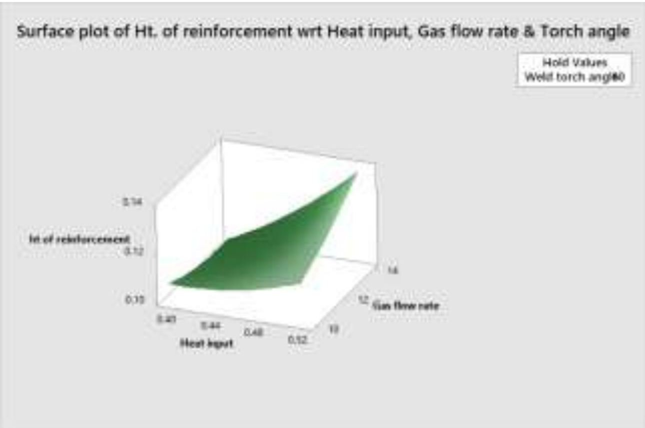

Fig -4: Surface Plot for Height of Reinforcement

Surface plot of height of reinforcement is shown in Figure 4. It is observed that height of reinforcement gradually increases from heat input of 0.40 kJ/mm onwards and reaches peak value at 0.51 kJ/mm. Consequently, it increases from gas flow rate of 10 lt/min and reaches maximum height at around 13 lt/min.

Analysis of Variance (ANOVA) was performed in measuring contribution of each input parameter on height of reinforcement as shown in Table 9.

Table-9: ANOVA Table of Height of Reinforcement

Source	DF	Adj SS	Adj MS	F-Value	P-Value
Model	9	0.006490	0.000721	14.76	0.000
Linear	3	0.005525	0.001842	37.71	0.000
Heat input	1	0.001277	0.001277	26.14	0.000
Gas flow rate	1	0.000168	0.000168	3.44	0.093
Weld torch angle	1	0.004080	0.004080	83.54	0.000
Square	3	0.000354	0.000118	2.42	0.127
Heat input*Heat input	1	0.000023	0.000023	0.46	0.512
Gas flow rate*Gas flow rate	1	0.000010	0.000010	0.20	0.668
Weld torch angle*Weld torch angle	1	0.000311	0.000311	6.37	0.030
2-Way Interaction	3	0.000610	0.000203	4.16	0.037
Heat input*Gas flow rate	1	0.000392	0.000392	8.03	0.018
Heat input*Weld torch angle	1	0.000018	0.000018	0.37	0.557
Gas flow rate*Weld torch angle	1	0.000200	0.000200	4.09	0.071
Error	10	0.000488	0.000049		
Lack-of-Fit	5	0.000218	0.000044	0.81	0.589
Pure Error	5	0.000270	0.000054		
Total	19	0.006978			

Model Summary: R-sq: 93.00%

It was observed that both heat input and weld torch angle with P-values of 0.000 (<0.05) each have considerable effect on height of reinforcement. Gas flow rate with a P-value of 0.093 (>0.05), has no effect on height of reinforcement. Also, R-sq value of 93.00%, indicates that the model is a good fit.

3.3 Bead Width

The Bead width for each combination of the input factors was measured. Nominal value of bead width is recommended. The detailed measurements are depicted in Table 10 and Table 11.

Table -10: Measured values of Bead Width

Sl. No.	Arc Current		Weld voltage	Weld speed (mm/s)	Heat input	Gas flow rate (lt/min)	Weld torch angle (degree)	Bead Width (mm)
	OC	CC						
1	100	102	10.6	2.18	0.389	10	45	3.654
2	140	141	11.3	2.18	0.510	10	45	3.145
3	100	101	10.6	2.18	0.389	14	45	3.894
4	140	142	11.3	2.18	0.510	14	45	3.013
5	100	100	10.6	2.18	0.389	10	75	5.632
6	140	141	11.3	2.18	0.510	10	75	4.248

Table -11: Measured values of Bead Width

Sl. No.	Arc Current (A)		Weld voltage (V)	Weld speed (mm/s)	Heat input (kJ/mm)	Gas flow rate (lt/min)	Weld torch angle (degree)	Bead Width (mm)
	OCC	CCC						
7	100	101	10.6	2.18	0.389	14	75	5.112
8	140	142	11.3	2.18	0.510	14	75	4.513
9	100	100	10.6	2.18	0.389	12	60	4.827
10	140	141	11.3	2.18	0.510	12	60	3.738
11	120	122	11.2	2.18	0.462	10	60	3.389
12	120	121	11.2	2.18	0.462	14	60	3.516
13	120	1211	11.2	2.18	0.462	12	45	3.231
14	120	121	11.2	2.18	0.462	12	75	4.262
15	120	121	11.2	2.18	0.462	12	60	3.917
16	120	122	11.2	2.18	0.462	12	60	3.568
17	120	121	11.2	2.18	0.462	12	60	3.712
18	120	121	11.2	2.18	0.462	12	60	3.687
19	120	122	11.2	2.18	0.462	12	60	3.472
20	120	121	11.2	2.18	0.462	12	60	3.326

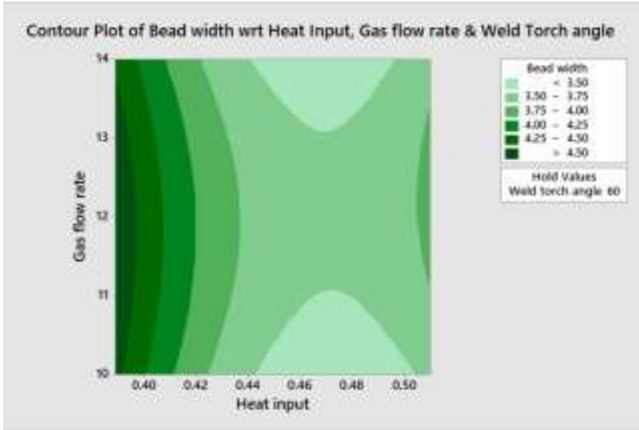

Fig -5: Contour Plot for Bead Width

Contour plot of bead width is shown in Figure 5. Weld torch angle is kept constant at 60º. It was observed that nominal bead width (<3.50 mm) was obtained at heat input of 0.45-0.51 kJ/mm at gas flow rates of 10-11 lt/min and 13-14 lt/min.

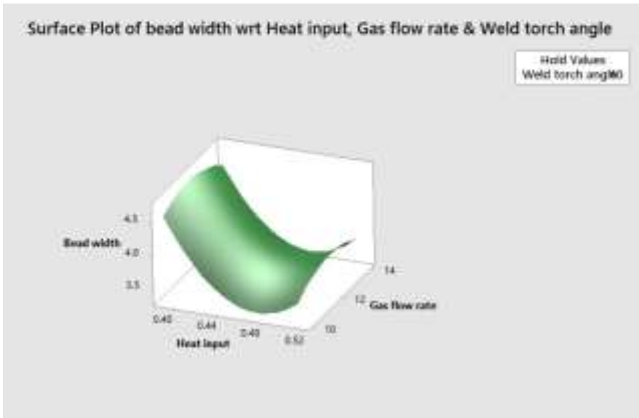

Fig -6: Surface Plot for Bead Width

Surface plot of bead width is shown in Figure 6. It is observed that bead width gradually decreases from heat input of 0.40 kJ/mm onwards and reaches lowest value at 0.48 kJ/mm. It then again rises towards the end. For gas flow rate, bead width increases from 10 lt/min onwards and reaches maximum at 12 lt/min and then decreases slightly towards the end.

Analysis of Variance (ANOVA) was performed in measuring contribution of each input parameter on bead width as shown in Table 12.

Table-12: ANOVA Table of Height of Reinforcement

Source	DF	Adj SS	Adj MS	F-Value	P-Value
Model	9	0.006490	0.000721	14.76	0.000
Linear	3	0.005525	0.001842	37.71	0.000
Heat input	1	0.001277	0.001277	26.14	0.000
Gas flow rate	1	0.000168	0.000168	3.44	0.093
Weld torch angle	1	0.004080	0.004080	83.54	0.000
Square	3	0.000354	0.000118	2.42	0.127
Heat input*Heat input	1	0.000023	0.000023	0.46	0.512
Gas flow rate*Gas flow rate	1	0.000010	0.000010	0.20	0.668
Weld torch angle*Weld torch angle	1	0.000311	0.000311	6.37	0.030
2-Way Interaction	3	0.000610	0.000203	4.16	0.037
Heat input*Gas flow rate	1	0.000392	0.000392	8.03	0.018
Heat input*Weld torch angle	1	0.000018	0.000018	0.37	0.557
Gas flow rate*Weld torch angle	1	0.000200	0.000200	4.09	0.071
Error	10	0.000488	0.000049		
Lack-of-Fit	5	0.000218	0.000044	0.81	0.589
Pure Error	5	0.000270	0.000054		
Total	19	0.006978			

Model Summary: R-sq: 93.00%

It was observed that both heat input and weld torch angle with P-values of 0.000 (<0.05) each have considerable effect on bead width. Gas flow rate with a P-value of 0.978 (>0.05), has no effect on bead width. Also, the R-sq value being high, i.e. 94.54%, it indicated that the model is a good fit.

4. Conclusions

In this experimental investigation, the Response Surface Methodology (RSM) design of experiment of Central Composite Design was utilized to investigate the weldability of Al-8%SiC metal matrix composite by TIG welding without using any filler metal, i.e. autogeneous and pure Argon of 99.99% purity as the shielding gas. The following conclusions were inferred-

1. Both Root Gap and Weld Torch Angle have significant effect on the depth of penetration with P-value of 0.000 for ANOVA.
2. The weld torch angle had more effect than root gap on Height of Reinforcement. The Reinforcement Height should be positive but of nominal value which indicate effective bead formation. The nominal value was obtained at Root gap of 0.75-1.36 mm and Weld torch angle of 45-53°.
3. Also, the weld torch angle had more effect than root gap on Weld Bead Width. The bead width should be as nominal as possible, which indicate effective bead formation. The nominal value was obtained over the range of 0.68-1.36 mm of Root Gap and Weld Torch Angle of 45-48°.
4. Optimal weld condition was obtained at heat input of 0.510 kJ/mm, gas flow rate of 14 l/min and weld torch angle of 45°.
5. The corresponding depth of penetration being 1.768 mm, bead width of 3.013 mm and height of reinforcement of 0.114 mm.

References

[1] Pichumani, S., Srinivasan, R., Ramamoorthi, V., Optimization of pulsed current TIG welding parameters on Al-SiC MMC to achieve max. bending strength, Advances in Natural and Applied Sciences, 16, (2017), pp.416-422

[2] Pichumani, S., Srinivasan, R., Ramamoorthi, V., Mechanical properties, thermal properties and microstructure characteristics of Al-8% SiC composite welded using pulsed TIG welding, Journal of Mechanical Sciences & Technology, Springer, 32, (2018), pp.1713-1723

[3] El-Sabbagh, A., Soliman, M., Taha, M., Palkowski, H., Hot rolling behaviour of stir-cast Al 6061 and Al 6082 alloys - SiC fine particulates reinforced composites, J. Mater. Process. Technol.,212, (2012), pp. 497-508

[4] Jahangiri, A., Idris, M.H., Farahan, S., Investigation on TIG welding of in-situ Al-15 and 20 Mg2Si composites with an Al-Si filler, Journal of Composite Material, 47, (2013), pp. 1283-1291

[5] Sabbagh, E., Soliman, M., Taha, M., Palkowski, H., Hot rolling behaviour of stir-cast Al 6061 and Al 6082 alloys - SiC fine particulates reinforced composites, J. Mater. Process. Technol, 212, (2012), pp.497-508

[6] Ravisankar, A., Velaga, S.G., Rajput, S.G., Venugopal, S., Influence of welding speed and power on residual stress during gas tungsten arc welding (GTAW) of thin sections with constant heat input: A study using numerical simulation and experimental validation, Journal of Manufacturing Processes, 16, (2014), pp. 200-211

[7] Ukitaand, K., Shimizu, K., Effects of shielding gas flow properties on ultra-high-speed DCEN TIG welding of ultra-thin aluminium sheets., Welding International, 9, (1995), pp.876-883

[8] Aravind, S., Das, A.D., An examination on GTAW samples of 7-series aluminium alloy using response surface methodology, Materials Today: Proceedings, 37, (2021), pp.614-620

[9] Pichumani, S., Srinivasan, R., Ramamoorthi, V., Investigation of Micro Hardness, Cooling Rate and Microstructure of ATIG Welded samples of Al-SiC composite, MATEC Web of Conferences, 151, 01002 (2018)

[10] Pichumani, S., Srinivasan, R., Ramamoorthi, V., Optimization of pulsed current TIG welding parameters on Al-SiC MMC to achieve max. bending strength, Advances in Natural and Applied Sciences, 16, (2017), pp.416-422

[11] Sivachidambaram, P., Balachandar, K., Optimization of Pulsed Current TIG Welding Parameters on Al-SiC Metal Matrix Composite – An Empirical Approach, Indian Journal of Science and Technology, (2015), 8(17)

[12] Pichumani,S., Raghuraman, S., Venkaraman, R., Correlation Between Microstructure and Microhardness on Al-SiC Composite Welded using Pulsed Current TIG Welding, ARPN Journal of Engineering and Applied Sciences, 10 (2015), pp.8141-8149

[13] Jayashree, P.K., Gowrishankar, M.C., Sharma, S., Shetty, R., Hiremath, P., Shettar, M., The effect of SiC content in aluminium-based metal matrix composites on the microstructure and mechanical properties of welded joints, Journal of Materials Research and Technology, 12 (2021), pp. 2325-2339

[15] Logsdon, W.A., Liaw, P.K., Tensile, fracture toughness and fatigue crack growth rate properties of silicon carbide whisker and particulate reinforced aluminium metal matrix composites, Engineering Fracture Mechanics, 24(5) (1986), pp.737-751

[16] Hong, S.J., Kim, H.M., Huh, D., Suryanarayana, C., Chun, B.S., Effect of clustering on the mechanical properties of SiC particulate-reinforced aluminium alloy 2024 metal matrix composites, Materials Science and Engineering: A, 347(1-2), (2003), pp.198-204

[17] Saini, S., Singh, S., Singh, K., Singh, A., Some studies into weldability of rice husk ash aluminium matrix composites using TIG welding. Materials Today: Proceedings, 37, (2020), pp.614-620

[18] Li,H., Wang, F., Lu, S., Sun, C., He, W., Han, X., Volodymyr,S., Study of Pulsed DC TIG Welded Joint's Properties of Al3Zr/A356 Particle-Reinforced Aluminium Matrix Composite, International Journal of Metalcasting, 17, (2023), pp.2762-2771

[19] Bansal, A., Kumar, M.S., Shekhar, I., Chauhan, S., Bhardwaj, S., Effect of welding parameter on mechanical properties of TIG welded AA6061. Materials Today: Proceedings, 37(2), (2021), pp. 2126-2131

[20] Aravind, S., Daniel Das, A., An examination on GTAW samples of 7-series aluminium alloy using response surface methodology. Materials Today: Proceedings, 37, (2021), pp. 614-620